JOURNAL OF THEORETICAL
AND APPLIED MECHANICS
1, 38, 2000

EQUATIONS OF MOTION AND DYNAMIC ANALYSIS OF PLANAR MANIPULATOR WITH FLEXIBLE LINK

JACEK OLEJAK

Department of Mechanics and Computer Methods, Technical University of Łódź in Bielsko-Biała
e-mail: jolejakpb.bielsko.pl

A mathematical model of a planar Sandia type manipulator is presented. The manipulator consists of two links: rigid and flexible, which are connected by rotary joints. The modal method was used to discretise the flexible link. The calculation results have been compared with the results of measurements. A good agreement has been achieved.

Key words: dynamics, control, manipulator

1. Introduction

A control of movements is one of the most interesting tasks of present manipulators. It is put into practice by control units of the drive system, which force relative movements in particular kinematics pairs. The task is more complicated, when the flexible links occur in a kinematics chain. It is very important, that at the design stage of the mechanism with flexible links, its behaviour during normal operation can be predicted.

When modelling flexible links in dynamic analysis, the finite element method (FEM) combined with the modal method (Du et al., 1992; Wojciech, 1996; Yuan et al., 1993) is often used. The modal method allows us to minimise the number of degrees of freedom of the structure.

In this work, the modal method is has been employed in discretisation of the beam-like flexible link in the two links SANDIA manipulator (Olejak, 1998), see Fig.1.

The deflection of the flexible link is assumed as follows

$$u(x',t) = \sum_{i=1}^{n} f_i(t)\eta_i(x') \tag{1.1}$$

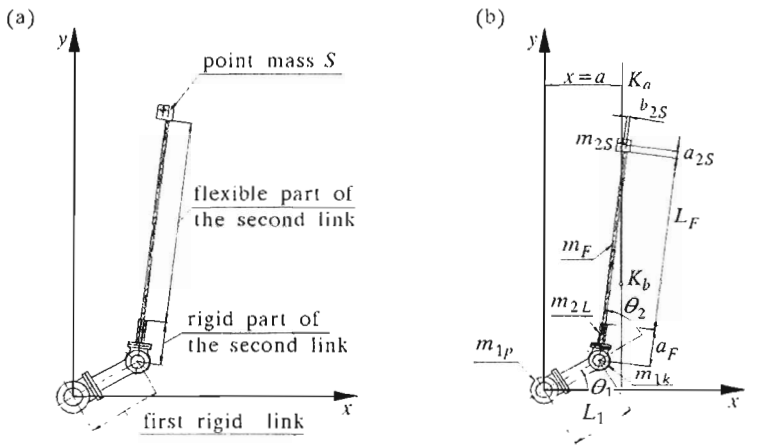

Fig. 1. Manipulator considered (a) elements of the manipulator, (b) model description

where

$f_i(t)$ – unknown time functions
$\eta_i(x')$ – known shape functions resulting from the FEM code
x' – local coordinate of the flexible link shown in Fig.2.

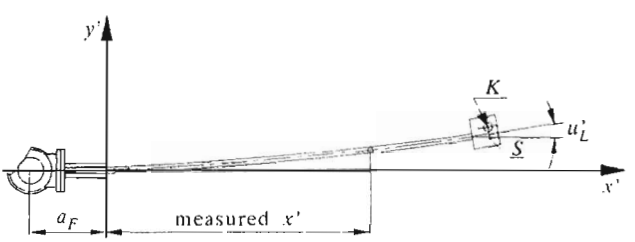

Fig. 2. Angle of deflection of the end point of the flexible link

2. Equations of the manipulator motion

The equations of the manipulator motion are derived from Langrange's equations of second order

$$\frac{d}{dt}\frac{\partial T}{\partial \dot{\boldsymbol{q}}} - \frac{\partial T}{\partial \boldsymbol{q}} + \frac{\partial V}{\partial \boldsymbol{q}} + \frac{\partial D}{\partial \dot{\boldsymbol{q}}} = \boldsymbol{Q} \tag{2.1}$$

where

$$\boldsymbol{q}^{\top} = [\theta_1, \theta_2, f_1, ..., f_m]$$

T – kinetic energy of the structure
V – potential energy of the structure
D – energy dissipation in the structure
$\boldsymbol{Q}$ – non-potential generalized forces.

There are $m+2$ generalized coordinates in the system:
θ_1 – rotation angle of the first rigid link
θ_2 – rotation angle of rigid part of the second link
$f_1, ..., f_m$ – functions corresponding to $1 \div m$ modes of the flexible link.

It is necessary to calculate the kinetic T and potential V energy of the structure to solve Eqs (2.1). In the work, the energy dissipation due to friction and internal damping is neglected.

The coordinates of flexible link points in basic system are as follows

$$\begin{aligned} x &= L_1 \cos\theta_1 + (a_F + x')\cos(\theta_1 + \theta_2) - u\sin(\theta_1 + \theta_2) \\ y &= L_1 \sin\theta_1 + (a_F + x')\sin(\theta_1 + \theta_2) + u\cos(\theta_1 + \theta_2) \end{aligned} \tag{2.2}$$

The local coordinates of the point S with the mass m_{2S} (Fig.2) can be written as

$$x'_S = A_S + \sum_{i=1}^{m} f_i\alpha_i \qquad y'_S = B_S + \sum_{i=1}^{m} f_i\beta_i \tag{2.3}$$

where

$$A_S = a_F + L_F + a_{2S} \qquad \alpha_i = -b_{2S}\eta'_i(L)$$

$$B_S = b_{2S} \qquad \beta_i = \eta_i(L) + a_{2S}\eta'_i(L)$$

The coordinates of this point in the inertial coordinate system are

$$\begin{aligned} x_S &= L_1 \cos\theta_1 + x'_S\cos(\theta_1 + \theta_2) - y'_S\sin(\theta_1 + \theta_2) \\ y_S &= L_1 \sin\theta_1 + x'_S\sin(\theta_1 + \theta_2) + y'_S\cos(\theta_1 + \theta_2) \end{aligned} \tag{2.4}$$

The kinetic energy of the structure is represented by the formula

$$
\begin{aligned}
T &= \frac{1}{2}I_1\dot{\theta}_1^2 + \frac{1}{2}(\dot{\theta}_1+\dot{\theta}_2)^2\Big[I_2 + \sum_{i=1}^{m} f_i w_i^* + \sum_{i=1}^{m} f_i \sum_{j=1}^{m} f_j \overline{m}_{ij}\Big] + \\
&+ \frac{1}{2}\sum_{i=1}^{m}\dot{f}_i \sum_{j=1}^{m}\dot{f}_j\overline{m}_{ij} + \dot{\theta}_1 \sum_{i=1}^{m} f_i(\overline{a}_i \sin\theta_2 + \overline{b}_i\cos\theta_2) + \\
&+ \dot{\theta}_1(\dot{\theta}_1+\dot{\theta}_2)\Big[A\sin\theta_2 + B\cos\theta_2 + \sum_{i=1}^{m} f_i(\overline{a}_i\cos\theta_2 - \overline{b}_i\sin\theta_2)\Big] + \\
&+ (\dot{\theta}_1+\dot{\theta}_2)\Big[\sum_{i=1}^{m} f_i\overline{v}_i + \sum_{i=1}^{m}\dot{f}_i\sum_{j=1}^{m} f_j u_{ij}^*\Big]
\end{aligned}
\tag{2.5}
$$

where

$$
\begin{aligned}
&I_1 = I_I + m_{1p}\Big[\frac{1}{12}l_1^2 + \Big(a_R + \frac{1}{2}l_1\Big)^2\Big] + (m_{1k} + m_{2L} + m_F + m_{2S})L_1^2 \\
&I_2 = \frac{1}{3}\rho_F F_F[(a_F+L_F)^3 - a_F^3] + I_{II} + m_{2S}(A_S^2 + B_S^2) \\
&\overline{m}_{ij} = m_{ij} + m_{2S}(\alpha_i\alpha_j + \beta_i\beta_j) \qquad m_{ij} = \int_{m_F}\eta_i\eta_j\, dm_F \\
&\overline{a}_i = m_{2S}L_1\alpha_i \qquad \overline{b}_i = L_1 a_i + m_{2S}L_1\beta_i \\
&A = -m_{2S}L_1 B_S \qquad B = m_{2S}L_1 A_S + L_1 S_F \\
&\overline{v}_i = b_i + m_{2S}(A_S\beta_i - B_S\alpha_i) \qquad u_{ij}^* = m_{2S}(-\alpha_i\beta_j + \alpha_j\beta_i) \\
&S_F = \int_{m_F}(a+x')\, dm_F \qquad w_i^* = 2m_{2k}(A_k\alpha_i + B_k\beta_i)
\end{aligned}
$$

In the considered case, the potential energy of gravity is neglected since both the links move in planes perpendicular to the direction of acceleration of gravity.

Thus, the potential energy of the structure is equal to the deflection energy of the flexible link

$$
V = \frac{1}{2}\boldsymbol{q}_F^{\top}\mathbf{K}^{ff}\boldsymbol{q}_F \qquad \boldsymbol{q}_F^{\top} = [f_1, ..., f_m] \tag{2.6}
$$

where $\mathbf{K}^{ff}$ is the stiffness matrix of the flexible link, elements of which are calculated from the formula

$$
K_{ij}^{ff} = \int_0^{L_F} EI_F\frac{d^2\eta_i}{dx^2}\frac{d^2\eta_j}{dx^2}\, dx \qquad i,j = 1, ..., m
$$

After transformations, the equations of manipulator motion can be rewritten in the following general form

$$\mathbf{A}\ddot{\boldsymbol{q}} + \mathbf{B}\dot{\boldsymbol{q}} + \mathbf{C}\boldsymbol{q} = \boldsymbol{F} \tag{2.7}$$

however the non-zero elements of matrices $\mathbf{A}$, $\mathbf{B}$, $\mathbf{C}$ are given by the formulas

$$a_{11} = I_1 + I_2 + 2(A\sin\theta_2 + B\cos\theta_2) +$$
$$+ \sum_{i=1}^{m} f_i\Big(-2\bar{b}_i\sin\theta_2 + 2\bar{a}_i\cos\theta_2 + w_i^* + \sum_{j=1}^{m} f_j\overline{m}_{ij}\Big)$$
$$a_{12} = I_2 + A\sin\theta_2 + B\cos\theta_2 +$$
$$+ \sum_{i=1}^{m} f_i\Big(-\bar{b}_i\sin\theta_2 + \bar{a}_i\cos\theta_2 + w_i^* + \sum_{j=1}^{m} f_j\overline{m}_{ij}\Big)$$
$$a_{1k} = \overline{v}_k + \bar{a}_k\sin\theta_2 + \bar{b}_k\cos\theta_2 + \sum_{i=1}^{m} f_i u_{ki}^* \qquad k = 3, ..., m+2$$
$$a_{22} = I_2 + \sum_{i=1}^{m} f_i\Big(w_i^* + \sum_{j=1}^{m} f_j\overline{m}_{ij}\Big)$$
$$a_{2k} = \overline{v}_k + \sum_{i=1}^{m} f_i u_{ki}^* \qquad k = 3, ..., m+2$$
$$a_{k1} = \overline{v}_k + \bar{a}_k\sin\theta_2 + \bar{b}_k\cos\theta_2 + \sum_{i=1}^{m} f_i u_{ki}^* \qquad k = 3, ..., m+2$$
$$a_{k2} = \overline{v}_k + \sum_{i=1}^{m} f_i u_{ki}^* \qquad k = 3, ..., m+2$$
$$a_{ki} = \overline{m}_{ki} \qquad i, k = 3, ..., m+2$$
$$b_{11} = \dot{\theta}_2\Big[A\cos\theta_2 - B\sin\theta_2 + \sum_{i=1}^{m} f_i\Big(-\bar{b}_i\cos\theta_2 - \bar{a}_i\sin\theta_2\Big)\Big] +$$
$$+ \sum_{i=1}^{m} \dot{f}_i\Big(w_i^* - \bar{b}_i\sin\theta_2 + \bar{a}_i\cos\theta_2 + \sum_{j=1}^{m} f_j\overline{m}_{ij}\Big)$$
$$b_{12} = (\dot{\theta}_1 + \dot{\theta}_2)\Big[A\cos\theta_2 - B\sin\theta_2 + \sum_{i=1}^{m} f_i\Big(-\bar{b}_i\cos\theta_2 - \bar{a}_i\sin\theta_2\Big)\Big] +$$
$$+ \sum_{i=1}^{m} \dot{f}_i\Big(w_i^* - \bar{b}_i\sin\theta_2 + \bar{a}_i\cos\theta_2 + \sum_{j=1}^{m} f_j\overline{m}_{ij}\Big)$$
$$b_{1i} = (\dot{\theta}_1 + \dot{\theta}_2)\Big(\sum_{j=1}^{m} f_j\overline{m}_{ij} + \bar{a}_i\cos\theta_2 - \bar{b}_i\sin\theta_2\Big) + \sum_{j=1}^{m} \dot{f}_j u_{ij}^*$$
$$i = 3, ..., m+2$$

$$b_{21} = -\dot{\theta}_1\Big[A\cos\theta_2 - B\sin\theta_2 + \sum_{i=1}^{m} f_i\Big(-\bar{b}_i\cos\theta_2 - \bar{a}_i\sin\theta_2\Big)\Big] +$$
$$+\sum_{i=1}^{m}\dot{f}_i\Big(w_i^* + \sum_{j=1}^{m} f_j\overline{m}_{ij}\Big)$$
$$b_{22} = \sum_{i=1}^{m}\dot{f}_i\sum_{j=1}^{m} f_j\overline{m}_{ij}$$
$$b_{2i} = (\dot{\theta}_1 + \dot{\theta}_2)\sum_{j=1}^{m} f_j\overline{m}_{ij} + \sum_{j=1}^{m}\dot{f}_j u_{ij}^* \qquad i = 3, ..., m+2$$
$$b_{k1} = (\dot{\theta}_1 + \dot{\theta}_2)\Big(-\frac{1}{2}w_k^* - \sum_{j=1}^{m} f_j\overline{m}_{kj}\Big) + \dot{\theta}_1(-\bar{a}_k\cos\theta_2 + \bar{b}_k\sin\theta_2) +$$
$$+2\sum_{i=1}^{m}\dot{f}_i u_{ki}^* \qquad k = 3, ..., m+2$$
$$b_{k2} = (\dot{\theta}_1 + \dot{\theta}_2)\Big(-\frac{1}{2}w_k^* - \sum_{j=1}^{m} f_j\overline{m}_{kj}\Big) + 2\sum_{i=1}^{m}\dot{f}_i u_{ki}^* \qquad k = 3, ..., m+2$$
$$c_{ij} = k_{ij}^{ff} \qquad i, j = 3, ..., m+2$$
$$\boldsymbol{F} = [\tau_1, \tau_2, 0, ..., 0]^\top$$

τ_1, τ_2 – torque moments acting on links 1 and 2.

Eqs (2.7) are the set of $m+2$ non-linear ordinary second order equations, which can be solved by means of any of numerical method. The newmark method with an iterative procedure is applied in the present contribution.

3. Comparison between the experimental and calculation results

Both the calculations and experiments were performed for the manipulator, shown in Fig.3. The TestPoint software was used to control the manipulator.

It is assumed, that the expected trajectory of the manipulator with rigid links motion is the straight line $x_k = a = 0.478\,\mathrm{m}$ and, that in the initial (a) and final (b) coordinates of the point K are also equal; i.e., $y_k|_{t=t_a} = 2.1\,\mathrm{m}$ and $y_k|_{t=t_b} = 1.2\,\mathrm{m}$ (Fig.4a), respectively. The links were: lengths rigid $L_1 = 0.478\,\mathrm{m}$, flexible $L_F = 1.725\,\mathrm{m}$ (Fig.4b).

In the work the values of parameters $t_a = 0$; $t_b = 3\,\mathrm{s}$ were taken respectively. The functions $\dot{\theta}_1$, $\ddot{\theta}_1$ and $\dot{\theta}_2$, $\ddot{\theta}_2$, which are used both in experiments and calculations, are shown in Fig.5.

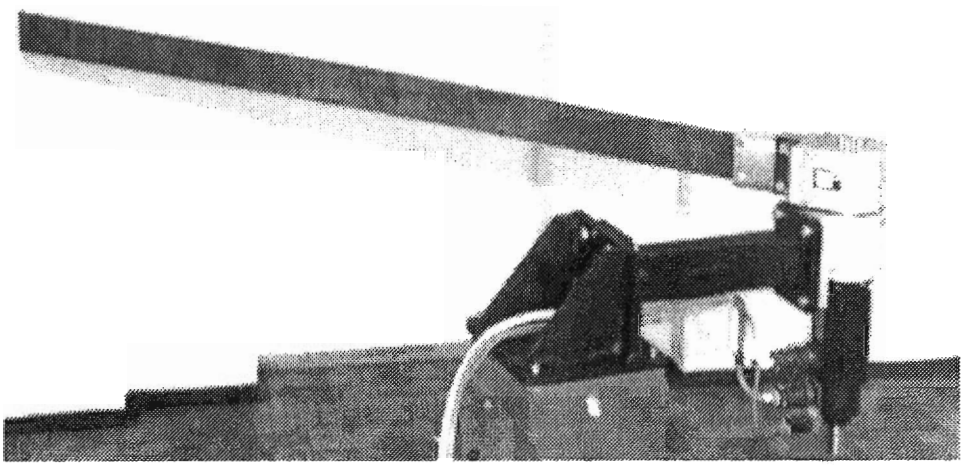

Fig. 3. General view of the manipulator

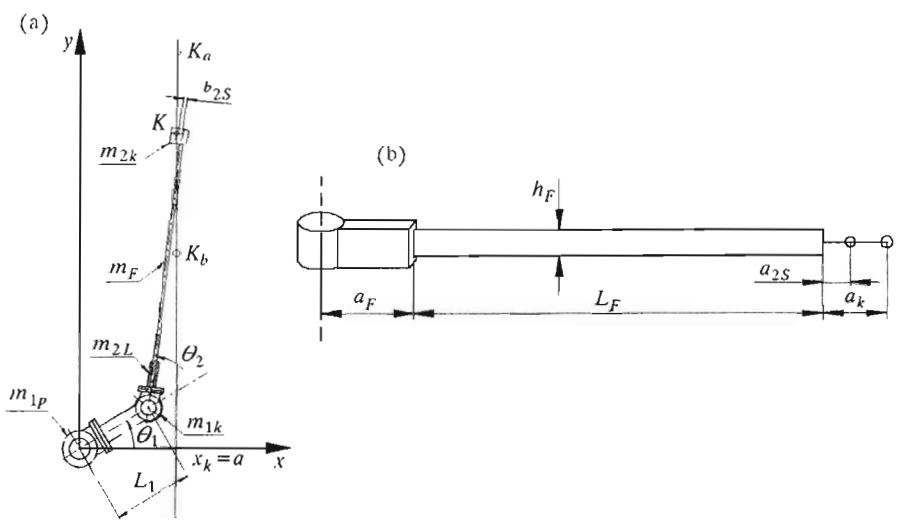

Fig. 4. Variables used for description of the manipulator (a) main parameters, (b) parameters of the flexible link

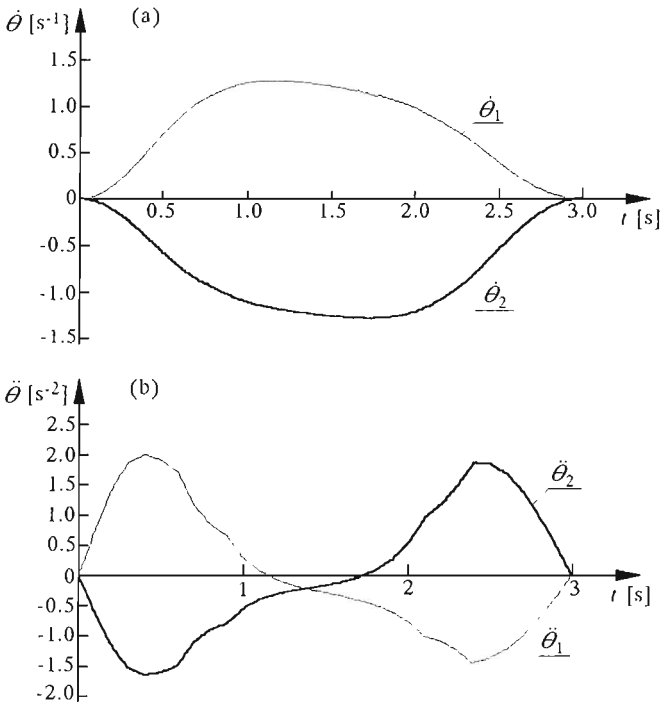

Fig. 5. Courses of the angulars velocities and accelerations in joints

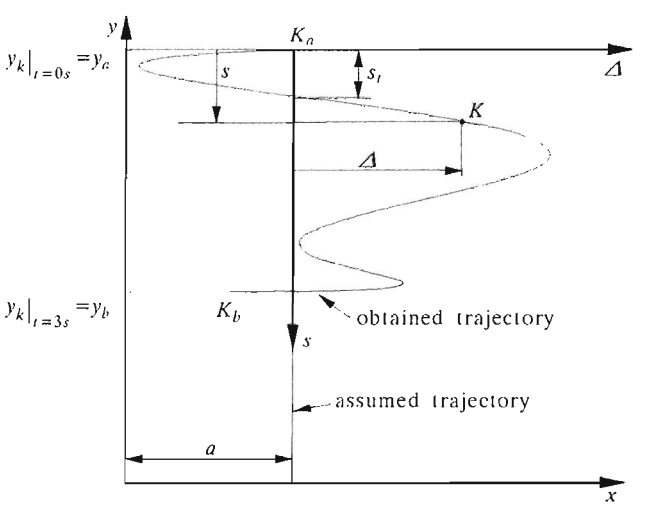

Fig. 6. Notation of variables used in figures

The courses of θ_1 and θ_2 are obtained solving the inverse kinematics problem for the manipulator with rigid links, taking into account the fact that the point K of rigid manipulator moves from K_a to K_b along the straight line $x = a$.

In order to determine the influence the number of modes m exerts on the result accuracy calculations were made for the above mentioned data and functions θ_1 and θ_2, shown in Fig.5.

In the paper the following notation is used (Fig.6)

s – displacement of the point K

Δ – deflection of the point K with respect to the trajectory (the straight line $x = a$).

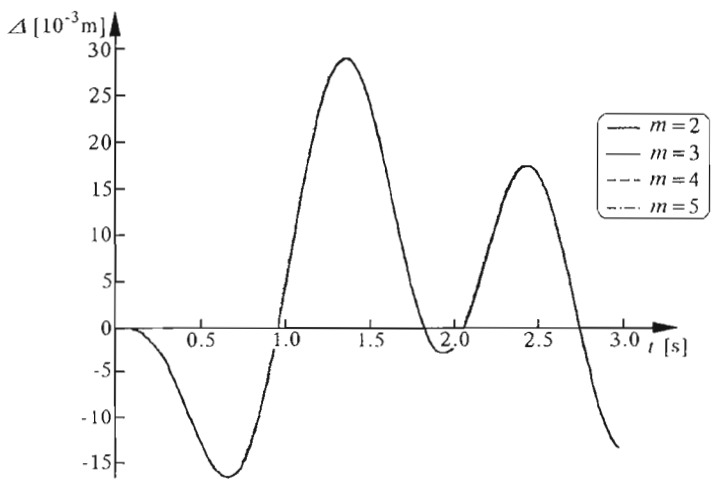

Fig. 7. Influence of the number of modes on the course of function $\Delta(t)$

In Fig.7 the courses of function $\Delta(t)$ for different values of the parameter m, are shown. It is assumed, that $n = 12$ (n is the number of finite elements, into which the flexible link was divided). The differences are so small, they can be hardly seen on the scale of this figure.

In Fig.8 the differences $\Delta\big|_{n=12,\, m=5} - \Delta\big|_{n=12,\, m=i}$ between the results obtained for $m = 5$ and $i = 2, 3, 4$, respectively, are shown.

It could be noticed, that the difference which does not exceed 0.015 mm (for deflection of about 25 mm of the flexible link) is just obtained for a number of the modes, which equals 3.

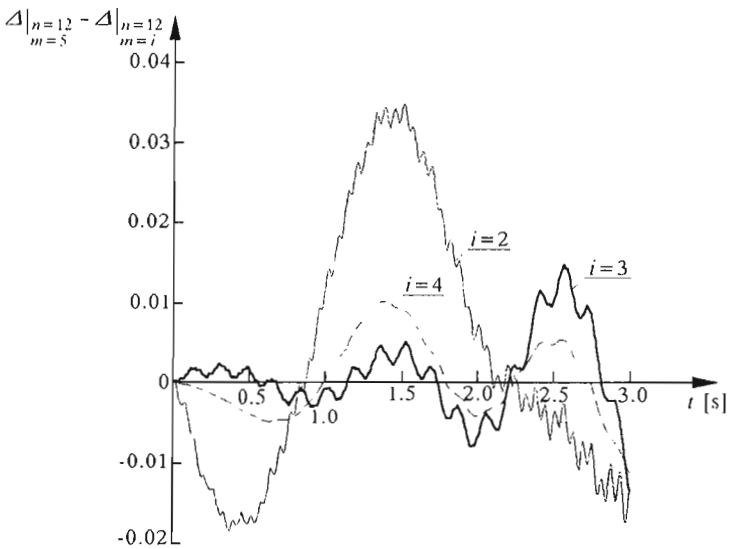

Fig. 8. Influence of the number of modes on the differences between $\Delta(t)\big|_{n=12,\ m=5}$ and $\Delta(t)\big|_{n=12,\ m=2,3,4}$

Then, in calculations we take the number of modes $m = 3$, which allows for the results accurate enough.

As it was mentioned above, the numerical model was verified also on an experimental stand. The trajectory of the point K was registered for the driving functions θ_1 and θ_2, which correspond to the curves shown in Fig.6.

In order to assess, whether the experiment and calculation courses of deflection of the point K are consistent, the following parameters of coincidence are suggested:

- s_{+}^{-} – value of the coordinate s, for which, the function $\Delta(s)$ for the first time changes its sign from the negative to positive value
- $\Delta_{\max}$ – maximal positive deflection of the point K of the flexible link with respect to the straight line $x = a$
- Δ_s – average value of deflection

$$\Delta_s = \frac{1}{t_b - t_a} \int_0^{y_b - y_a} \Delta(s)\, ds$$

Table 1. Values of the parameters s_+^-, $\Delta_{\max}$, Δ_s

Number of experiment p_i	s_+^-	+/−	$\Delta_{\max}$	+/−	Δ_s	+/−
1	0.162	+	26.041	+	2.606	+
2	0.164	+	27.170	+	2.589	+
3	0.152	−	28.780	+	3.193	−
4	0.158	+	25.000	−	2.573	+
5	0.150	−	27.347	+	3.123	−
6	0.167	+	29.407	−	3.021	+
7	0.168	+	29.388	−	2.950	+
8	0.172	+	26.277	+	2.488	+
9	0.182	−	26.041	+	2.288	−
$\overline{x}$ average value	0.164		27.272		2.759	
σ standard deviation	0.0033		0.5337		0.1059	
calculation results	0.1656		26.234		2.446	

In Table 1 the values of the parameters for a series of 9 measurements are presented. In additional columns there are signs "−" or "+", which show whether the following condition is satisfied

$$\overline{x} - 3\sigma \leqslant x_i \leqslant \overline{x} + 3\sigma \tag{3.1}$$

where

x_i – measured value of variable
$\overline{x}$ – its average value
σ – standard deviation.

The standard deviation for the measurement is calculated according to the formula

$$\sigma = \sqrt{\frac{\sum_{i=1}^{p}(x_i - \overline{x})^2}{p(p-1)}} \tag{3.2}$$

where p – number of measurements.

Analysis of the results from Table 1 shows, that the condition (3.1), put into all three quantities s_+^-, $\Delta_{\max}$, Δ_s concurrently, is satisfied by measurements p_1, p_2, p_8, shown in Fig.9, in which, the result of calculation is also placed.

The calculated deflection from trajectory $x = a$ is compared with average of measurements in Fig.10.

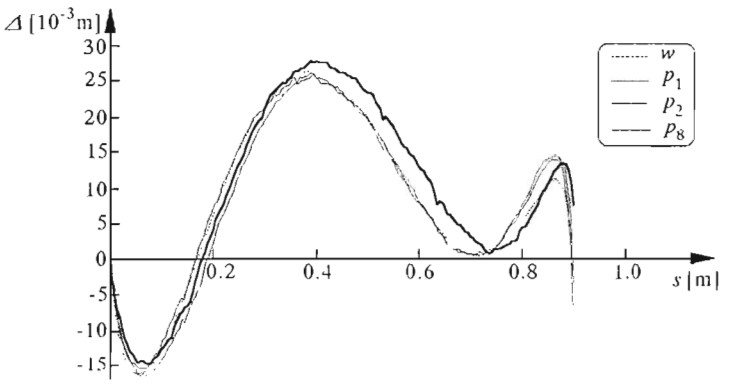

Fig. 9. Comparison between the calculation and measurement results in the case without an additional mass: w – calculation result; p_1, p_2, p_8 – measurement results

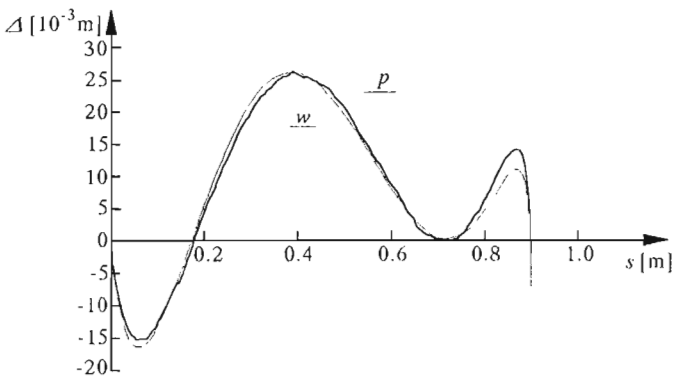

Fig. 10. Deflection course of the manipulator end from expected path: w – calculated course; p – average of measurements

The diagrams from Fig.9 and Fig.10 show good agreement between the calculation and measurement results.

Table 2. Average value of measurements and calculation result

Parameter	x_p average of measurements	x_t calculation results	ε error
s_+^-	0.166	0.1656	0.2%
$\Delta_{\max}$	26.496	26.234	1.0%
Δ_s	2.561	2.446	4.5%

In Table 2 are average values of measurements, calculation value and percentage errors.

Maximal difference between the values resulting from experiments on the test stand and calculated ones does not exceed 5% for the considered case.

4. Conclusions

The mathematical model does not include all features of the real manipulator. The phenomenon, connected with dynamic of the drive, flexibility and clearances existing in a real drive system, were neglected. The manipulator motion control realised on the test stand, did not provide accurate realisation of the calculated angular velocities for both links. It was mainly caused by application of the TestPoint software on a PC computer (operating system – Windows'95). The measurement results could correspond to the calculated ones in a better way, if a real time system would be used for control.

The results of calculations and measurements allow one to formulate the following conclusions:

- Sufficient accuracy of calculations, using the modal method was obtained for $m \geqslant 3$
- Comparison between the calculation and measurement results (Fig.9) proves nearly the same courses of the point K deflection from the calculated trajectory (relative error does not exceed 5% – Table 2).

References

1. DU H., HITCHINGS D., DARIES G.A., 1992, A Finite Element Structural Model of a Beam with an Arbitrary Mowing Base, Part I: Formulations, Part II: Numerical Examples and Solutions, *Finite Element in Analysis and Design*, **12**
2. OLEJAK J., 1998, Control of Motion of Manipulator with Flexible Links, PhD thesis, TU of Łódź in Bielsko-Biala (in Polish)
3. WOJCIECH S., 1996, Optimal Drive Courses for Manipulator with Finite Links, *VII International Congress on the Theory of Machines and Mechanisms, Proceedings*, 713-718, Liberec

4. YUAN B.S., BOOK W.J., HUGGINS J.D., 1993, Dynamics of Flexible Manipulator Arms: Alternative Derivations, and Characeristics for Control, *ASME Journal of Dynamics Systems, Measurement, and Control*, **115**, 394-404

Równania ruchu i dynamiczna analiza płaskiego manipulatora z podatnym członem

Streszczenie

W pracy przedstawiono model matematyczny płaskiego manipulatora typu SANDIA z podatnym członem. W modelowaniu podatnego członu zastosowano metodę modalną. Dokonano porównania wyników symulacji numerycznej z pomiarami na stanowisku badawczym. Błąd względny odchylenia, trajektorii wybranego punktu manipulatora, zmierzonego na stanowisku badawczym w odniesieniu do trajektorii otrzymanej analitycznie jest mniejszy od 5%.

Manuscript received June 11, 1999; accepted for print September 22, 1999